TEKSTİL VE MÜHENDİS

(Journal of Textiles and Engineer)

http://www.tekstilvemuhendis.org.tr

Comparative Analysis of Electrospun Uniaxial and Coaxial Nanofibers Properties

Elektro Lif Çekim Yöntemi ile Üretilen Tek ve Eş Eksenli Nanoliflerin Özelliklerinin Karşılaştırmalı Analizi

Nuray KIZILDAG

Sabancı University, Integrated Manufacturing Technologies Research and Application Center, Istanbul, Turkey

Online Erişime Açıldığı Tarih (Available online):1 Nisan 2021 (1 April 2021)

Bu makaleye atıf yapmak için (To cite this article):

Nuray KIZILDAG (2021): Comparative Analysis of Electrospun Uniaxial and Coaxial Nanofibers Properties, Tekstil ve Mühendis, 28: 121, 23-31.

For online version of the article: https://doi.org/10.7216/1300759920212812103

Araştırma Makalesi / Research Article

COMPARATIVE ANALYSIS OF ELECTROSPUN UNIAXIAL AND COAXIAL NANOFIBERS PROPERTIES

Nuray KIZILDAG*

Sabancı University, Integrated Manufacturing Technologies Research and Application Center, Istanbul, Turkey

Gönderilme Tarihi / Received: 30.12.2020
Kabul Tarihi / Accepted: 25.03.2021

ABSTRACT: Coaxial electrospinning, which is a modified electrospinning technique involving an arrangement of multiple solution feed systems, enable the production of multilayered nanofibers. In this study, multilayered nanofibers of polyamide 6 (core) / polycaprolactone (shell) containing silver nanoparticles in the core were produced by coaxial electrospinning method. UV-Visible spectra showed that the size of nanoparticles were about 10 nm and the content of nanoparticles were observed to be proportional to the precursor content added to the solvent. The obtained multilayered nanofibers were characterized in terms of morphology, chemical structure, and silver release properties. The multilayered nanofiber structure was confirmed by the selective dissolution and removal of shell layer. The increase in the PCL content of the multilayered nanofibers with the increase in the flow rate of the shell solution was confirmed by FTIR. The silver release profiles of the nanofibers were observed to be dependent on the nanofiber configuration, and silver content. Shell thickness was also an important parameter affecting the silver release properties for multilayered nanofibers.

Keywords: Antibacterial, coaxial electrospinning, controlled release, nanofiber.

ELEKTRO LİF ÇEKİM YÖNTEMİ İLE ÜRETİLEN TEK VE EŞ EKSENLİ NANOLİFLERİN ÖZELLİKLERİNİN KARŞILAŞTIRMALI ANALİZİ

ÖZET: Konvansiyonel elektro lif çekim yönteminin birden çok çözeltinin beslenmesine yönelik yapılan modifikasyonu ile elde edilen koaksiyal elektro lif çekim yöntemi, çok katmanlı nanoliflerin üretimini sağlayan bir yöntemdir. Bu çalışmada, koaksiyal elektro lif çekim tekniği kullanılarak öz kısmında gümüş nanopartiküller içeren polyamide 6 (öz) / polikaprolakton (kabuk) nanolifler üretilmiş ve elde edilen çok katmanlı nanolifler morfoloji, kimyasal yapı ve gümüş salım özellikleri açısından değerlendirilmiştir. UV-görünür bölge spektroskopisi, sentezlenen gümüş nanopartiküllerin 10 nm'den küçük olduğunu ve gümüş nanopartikül miktarının, çözeltiye eklenen prekursör miktarı ile orantılı olduğunu göstermiştir. PCL kabuk kısmının çözülerek uzaklaştırılması ve PA6 öz kısmının geride saf halde, nanolif formunda kalması ile koaksiyal nanolif yapısı doğrulanmıştır. Kabuk çözeltisinin besleme hızı arttırıldığında, nanolif yapısındaki PCL miktarı artmış ve FTIR spektrumunda PCL'e ait piklerin şiddetleri artmıştır. Nanoliflerin gümüş salım profillerinin nanolif konfigürasyonu, gümüş prekursör miktarı ve çok katmanlı nanoliflerde ayrıca kabuk kalınlığına bağlı olarak değiştiği görülmüştür.

***Anahtar Kelimeler*:** Antibakteriyel, koaksiyal elektro lif çekimi, kontrollü salım, nanolif.

***Sorumlu Yazar/Corresponding Author:** nuray.kizildag@sabanciuniv.edu*
***DOI:** https://doi.org/10.7216/1300759920212812103 www.tekstilvemuhendis.org.tr*

1. INTRODUCTION

Electrospinning is a process that uses electrostatic forces to produce nanofibers. The setup for the conventional electrospinning consists of a pump, which is used to feed the solution through the needle, a high voltage power supply, which is used to charge the electrospinning solution and create electric field between the tip of the needle and the collector, and a grounded collector, which is used to collect the nanofibers in the nanoweb form. In the electric field forming between the needle and the collector, a jet occurs when the electrostatic force overcomes the surface tension of the solution droplet and undergoes bending and whipping instability as a result of which the solvent evaporates and nanofibers form. Electrospun nanofibers have taken great interest due to their unique properties, ease of fabrication, and possibilities of functionalization [1-3].

In recent years, many modifications have been made in the basic electrospinning process in order to enhance the quality and improve the functionality of the resulting nanofibers. Coaxial electrospinning is one of these modifications, which attracted great attention. In the process of coaxial electrospinning, two polymer solutions are co-electrospun without direct mixing using a special coaxial needle. The setup for coaxial electrospinning is basically the same as the conventional electrospinning setup that is used for uniaxial electrospinning. The difference is that it contains two pumps to feed two different solutions through the needle. When voltage is applied to the coaxial needle, it deforms the compound droplet, which is at the tip of the needle. A jet is generated on the tip of the deformed droplet and a coaxial (core-shell) nanofiber is formed in the ideal case [4].

Coaxial nanofibers are reported to show great promise in a variety of applications. Unspinnable materials such as drugs, enzymes, etc. could be electrospun as the core of a fiber forming polymer [5-8]. In addition, it was used for the encapsulation of epoxy and amine curing agent within a polymer shell to produce coaxial nanofibers suitable for use in self-healing applications [8,9]. Nanowebs, which exhibited balanced thermal storage and releasing properties for thermo-regulating functions, were obtained using phase changing materials (PCM) in the core [10]. Fibers of unspinnable polymers could be obtained by using the unspinnable polymer as the core material and removing the shell layer after coaxial electrospinning [11]. With a similar approach, but removing the core material, it was possible to obtain hollow fibers [12,13]. Coaxial electrospinning was also used to improve the properties of the nanofibers. Biocompatible nanofibers with enhanced mechanical properties could be obtained [14-16]. Merkle et al. used coaxial electrospinning to fabricate nanofibers with gelatin in the shell and poly (vinyl alcohol) (PVA) in the core in order to derive mechanical strength from PVA and bioactivity from gelatin [14]. Pakravan et al. produced coaxial nanofibers of PEO as the core and chitosan as the shell [15]. Nguyen et al. prepared biodegradable non-woven mats of poly (lactic acid) (PLA) and chitosan (CS) by the coaxial electrospinning process. CS of high molecular weight could not be electrospun on its own because of its high viscosity in solution and its polycationic possession. The coaxial electrospinning method was able to facilitate the fabrication of double-layer PLA/CS composite nanofibers by employing a PLA layer in the core and a CS layer in the shell part. The PLA/CS core/shell composite nanofibers showed antibacterial activity against *Escherichia Coli* and were suggested for use as antibacterial materials in biomedical and filtration applications [16]. Coaxial nanofibers are widely employed in controlled drug delivery applications as they make it possible to control the release profiles of the drugs encapsulated in the coaxial nanofibers [17-20].

Silver has been the mostly used material to fight against bacteria, viruses, and other eukaryotic microorganisms. Moreover it is known that its use in the nanoscale dimensions maximizes its antibacterial effect due to the increase in number of particles per unit area with size reduction [21].

The rate and the amount of silver release are important factors for antibacterial performance of the nanofibers [22,23]. The cumulative amount of silver released, and the rate of release is dependent on the silver content. While higher AgNP content provides long-lasting antibacterial activity, it results in higher burst release and higher release rates, which bring no benefits. Although there are many studies in literature showing the production of AgNP loaded nanofibers with antibacterial properties [22-31], there are very limited number of studies performed for the finetuning of the silver release properties in order to get a lower silver release rate which will ensure the antibacterial activity to last longer. In this study, coaxial electrospinning containing AgNPs was suggested as a way of controlling the silver release properties. Uniaxial and coaxial nanofibers were produced changing the concentration of the silver precursor. For the coaxial nanofibers, the flow rate of the shell polymer solution was varied in order to control the release profiles of the nanofibers and assure sustained and controlled release properties.

2. MATERIALS AND METHOD

2.1 Materials

Polyamide 6 (PA6) (Sigma Aldrich, 181110, pellets, 3 mm), polycaprolactone (PCL) (Sigma Aldrich, 440744, Mn=80000), formic acid (Sigma Aldrich, F0507, 98%), acetic acid (Sigma Aldrich, 33209, 98%) were used as received in the electrospinning solutions. Silver nitrate ($AgNO_3$) (Alfa Aesar Premion, 10858, 99.9995% metals basis) was used as the precursor for the synthesis of AgNPs in the PA 6 solution.

2.2 Methods

Preparation of the solutions

18 wt.% PA 6 solution was prepared in 50:50 formic acid: acetic acid solvent mixture for the electrospinning of uniaxial PA 6 nanofibers. 8 wt.% PCL solution was prepared in 50:50 formic acid: acetic acid solvent mixture to be used as the shell solution in coaxial electrospinning. $AgNO_3$ were added to the required

amount of formic acid: acetic acid (50:50% mixture) and homogenized in ultrasonic bath at 50°C overnight. The required amount of PA 6 (18 wt.%) was added to this dispersion and dissolved by magnetically stirring at room temperature for 3 hours. Then the solutions containing $AgNO_3$ were exposed to UV-light for 4 hours for silver nanoparticle synthesis [23,32]. 300W Osram Ultra-Vitalux lamp was used as UV irradiation source. AgNP containing PA 6 solutions were used for uniaxial composite nanofiber electrospinning and as the core solution in the coaxial electrospinning.

Electrospinning

The uniaxial and coaxial nanofibers were produced on a lab-scale horizontal electrospinning setup with a generic flat stationary nanofiber collector using coaxial needle (Raméhart Custom Needle, 100-10-COAXIAL-2016, outer needle: 1.7 mm OD, inner needle: 0.9 mm OD). The schematic of the setup used for nanofiber production is presented in Figure 1.

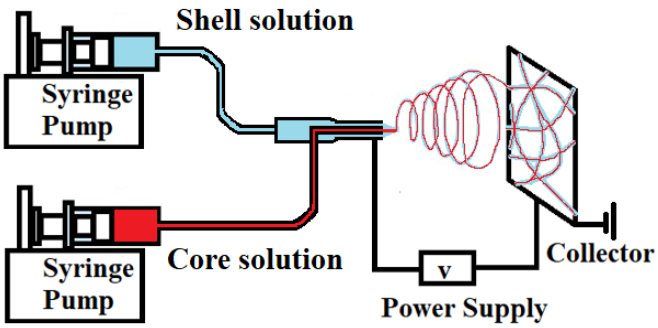

Figure 1. The schematic of the electrospinning setup used for nanofiber production.

To produce uniaxial PA 6 nanofibers and composite PA 6 nanofibers with silver nanoparticles, the prepared solutions were fed to the inner needle by a precisely controlled syringe pump (KD Scientific Pump Series 100). A high voltage power supply (Glassman High Voltage Series) was used to apply high voltage to the electrospinning solutions. The distance between the tip of the needle and the collector (TCD), the flow rate (FR) and the applied voltage were adjusted to obtain stable electrospinning and uniform nanofibers. To produce multilayered nanofibers, two pumps (KD Scientific Pump Series 100) were used to feed the core and shell solutions, respectively. A high voltage power supply (Glassman High Voltage Series) was used to apply high voltage to the outer needle. TCD, FRs of the solutions and the voltage were adjusted to obtain stable electrospinning and uniform coaxial nanofibers. Special care was taken to ensure stable electrospinning conditions and uniform deposition of the nanofibers. The nanofibers electrospun are listed in Table 1.

Extraction of PCL shell

The multilayered nanofiber webs of approximately 4 x 4 cm^2 in size were immersed into 20 mL of anisole to extract the PCL shell and confirm the multilayered fiber structure. Anisole was selected for selective dissolution of PCL [33] as it doesn't dissolve PA6. After refreshing the anisole three times over a day, the nanowebs were dried at room temperature until obtaining constant weight in subsequent weighings. The nanofibers were tested regarding their weight, average nanofiber diameter and chemical structure before and after anisole treatment.

Characterization

Lambda 900 spectrophotometer from Perkin-Elmer was used to obtain the UV-Visible spectra of 10 mg/l 100% PA solution and PA solutions prepared by adding 1 and 3 wt.% $AgNO_3$ in the 300-800 nm region with a resolution of 1 nm to confirm the formation of AgNPs.

The morphology of the nanofibers were analysed using scanning electron microscope (SEM, Jeol Quanta 200 FESEM). SEM images were taken at an accelarating voltage of 20 kV. Before SEM analysis, the samples were coated with gold using a sputter coater (Baljes Union SKD 030). The fiber diameters were measured using Image J. The average nanofiber diameters and the standard deviations were based 50 measurements per sample. Average nanofiber diameters were expressed as the mean ± standard deviation. The morphology of the fibers were also analysed in the same way after they were treated with anisole for the removal of PCL shell.

Table 1. The list of the nanofibers produced and the electrospinning parameters used in their production.

Sample Codes	Core solution	Shell solution	TCD (cm)	FR Core (mL/h)	FR Shell (mL/h)	Applied Voltage (kV)
S1	18 wt.% PA	*	6	1.5	*	21
S2	18 wt.% PA 6 - 1 wt.%$AgNO_3$	*	6	1.5	*	18
S3	18 wt.% PA 6 - 3 wt.%$AgNO_3$	*	6	1.5	*	18
S4	18 wt.% PA 6 - 1 wt.%$AgNO_3$	8 wt.% PCL	8	1.5	0.4	24
S5	18 wt.% PA 6 - 1 wt.%$AgNO_3$	8 wt.% PCL	8	1.5	1.4	27
S6	18 wt.% PA 6 - 3 wt.%$AgNO_3$	8 wt.% PCL	8	1.5	1.4	27

Fourier transform infrared (FTIR) spectrophotometer from Thermo Scientific was used to record absorption spectra of multilayered nanofibers in a range from 4000 to 400 cm^{-1} with a resolution of 4 cm^{-1}. 32 scans were taken for each experiment.

Atomic adsorption spectrometry (AAS) was used to characterize the AgNP containing nanofibers in terms of their silver release profiles. Distilled water was used as the release medium and 0.1 g of nanofiber sample was placed in 50 mL distilled water. The containers were sealed and agitated to ensure the complete immersion of the nanofiber sample, and then left for silver release at room temperature. 5 mL samples from the solutions were taken at specified immersion times (1st, 3rd, 8th, 10th, 20th and 30th day) and quantified for the silver content by means of ContrAA700 Graphite-Furnace Atomic Absorption Spectrometer. Silver ion release amounts were calculated by integration of the area under the characteristic absorbance peak of Ag which is 328.068 nm.

3. RESULTS AND DISCUSSION

3.1 UV-Visible Spectroscopy

UV-Visible Spectroscopy was used to control the formation of silver nanoparticles in the PA 6 solutions, which were first homogenized in ultrasonic bath at 50°C overnight and then exposed to UV-irradiation for 4 hours for silver nanoparticle synthesis. Silver nanoparticles show a strong absorption peak in the UV-visible range due to the discrete energy levels of electrons caused by the quantum size effect, which enables to make a rough estimation about the size of the nanoparticles obtained and quantitative analysis [23,34,35]. The UV-Vis spectra obtained are presented in Figure 2. While no peaks were observed in the UV-Vis spectrum of PA 6, the peaks observed at around 420 nm confirmed the formation of nanoparticles, which were 10 nm or less in size [23,34,35]. The maximum absorbance values increased from 0.51 to 1.64 when the $AgNO_3$ content increased from 1 wt.% to 3 wt.%.

3.2 Morphology

The process parameters were optimised to obtain uniform PA 6 nanofibers, composite PA 6 nanofibers with AgNPs and coaxial nanofibers. While the optimization processes for PA 6 nanofibers and composite nanofibers were relatively easier and based on literature information, coaxial electrospinning was observed to be more sensitive to process conditions and it required more effort to find optimum settings regarding core and shell flow rates, applied voltages and tip-to-collector-distances to be able to obtain a stable Taylor cone, which is a prerequisite for the stable coaxial electrospinning and uniform multilayered nanofibers. High flow rate of shell solution, high and/or low voltage resulted in phase separation during electrospinning. When the distance between the needle and the collector was small, web-like structures formed between the needle and the collector, which resulted in nonuniform nanofiber web formation. As either the flow rate or concentration of PCL shell solution increased, the tip-to-collector distance also had to be increased in order to obtain uniform coaxial nanofibers. Multilayered nanofibers with AgNP loaded PA 6 as the core and PCL as the shell were produced as listed in Table 1 after a detailed systematic optimization study. Representative SEM images of nanofibers are presented in Figure 3 with the average nanofiber diameters on the SEM images.

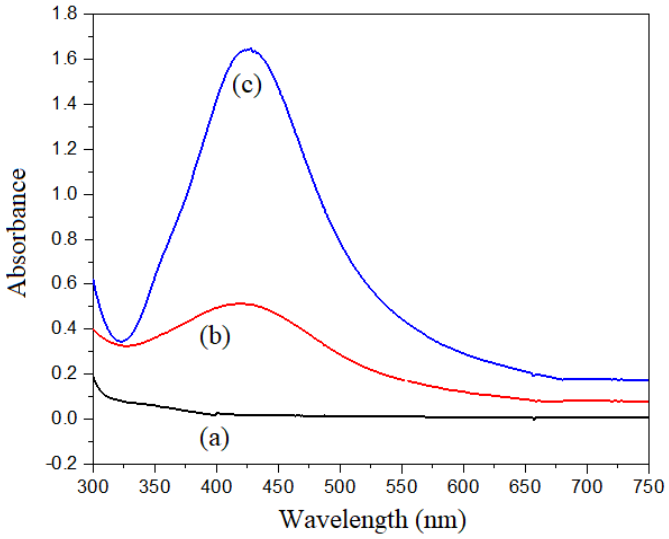

Figure 2. UV-Visible spectra of (a) 100% PA 6; (b) PA 6 - 1wt.%$AgNO_3$; (c) PA 6 - 3wt.%$AgNO_3$ solutions after AgNP synthesis via UV irradiation.

Uniform uniaxial PA 6 nanofibers with an average diameter of 221.70 nm were obtained. Decrease in average nanofiber diameter was observed when composite PA6 nanofibers were electrospun from AgNP containing solutions likely due to the increased stretching during electrospinning process. Coaxial nanofibers were produced using 18 wt. % PA 6 as the core and 8 wt. % PCL as the shell solutions and changing the shell flow rate and $AgNO_3$ concentration in the core solution. The multilayered nanofibers had smooth surfaces and were uniform in structure. Increase in the shell flow rate resulted in the formation of thicker coaxial nanofibers.

The coaxial nanofibers were treated with anisole for the selective extraction of PCL shell producing PA 6 nanofibers which were also characterized by SEM to confirm the multilayered morphology of the fibers obtained by coaxial electrospinning. SEM images of 100% PA 6 nanofibers and coaxial nanofibers taken after anisole treatment are shown in Figure 3. SEM images of (a) S1, (b) S2, (c) S3, (d) S4, (e)S5, (f) S6 nanofibers taken with 25000 magnification.Figure 4. The average nanofiber diameters are shown on the SEM images. The reduction in diameter of nanofibers and weight of the nanowebs after the anisole treatment are given in Table 2.

While no changes were observed on neat PA nanofibers after the anisole treatment, the smooth surfaces of coaxial nanofibers became rougher after the extraction of PCL shell by anisole treatment. The continuous fiber structure was preserved after PCL extraction, which confirmed the multilayered nanofiber morphology. Anisole treatment resulted in neither reduction nor increase in the diameter of the PA nanofibers. On the other hand, it resulted in a significant reduction in diameter of the coaxial nanofibers as a result of the removal of the PCL shell (Figure 4, Table 2). The weight reduction (%) of multilayered nanofibers (removed PCL amounts) by anisole treatment were proportional to their calculated PCL contents (Table 2). Higher reduction in average nanofiber diameter was observed for the nanofibers (S5 and S6) which were produced with higher shell flow rates (Figure 4, Table 2).

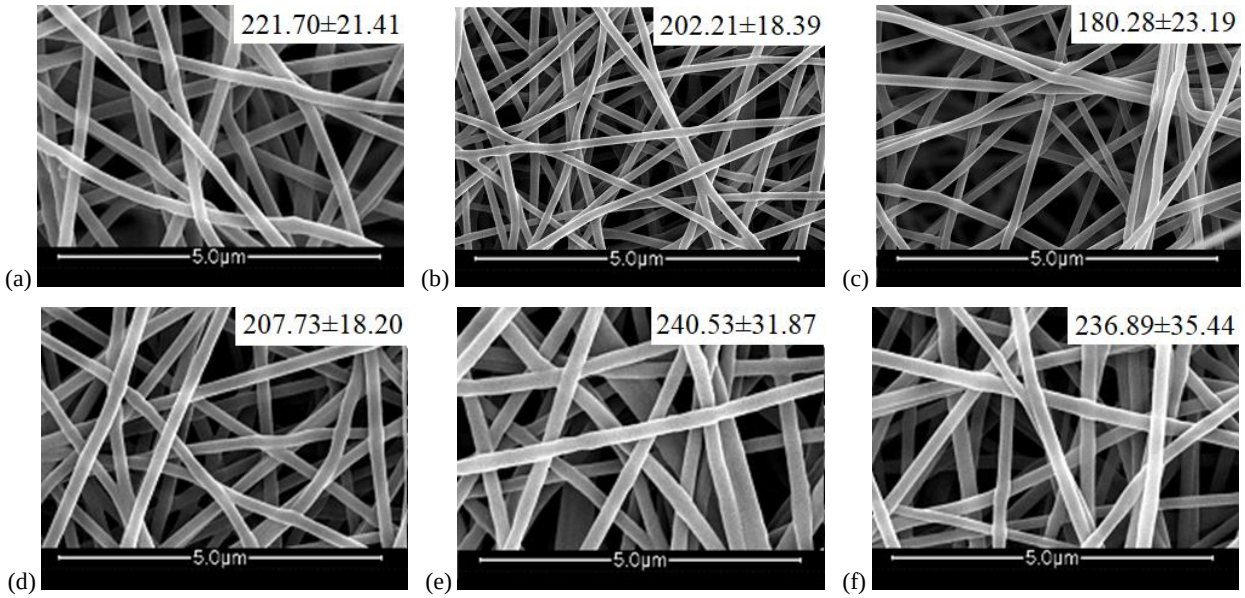

Figure 3. SEM images of (a) S1, (b) S2, (c) S3, (d) S4, (e)S5, (f) S6 nanofibers taken with 25000 magnification.

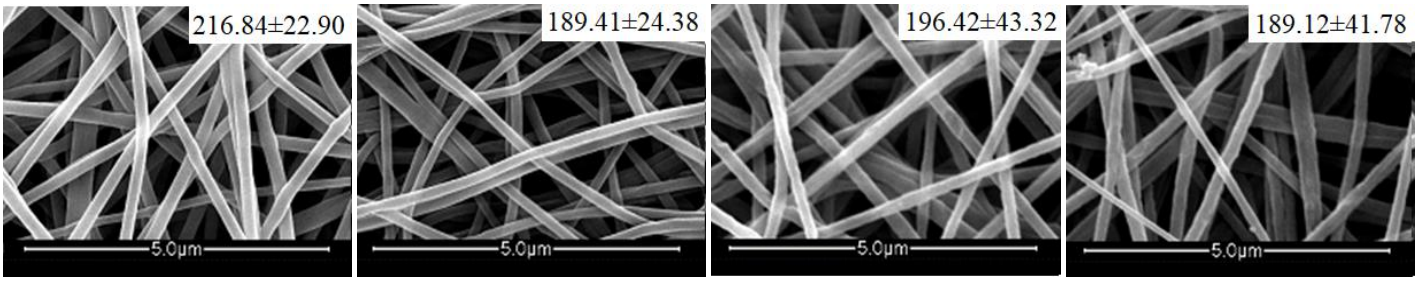

Figure 4. SEM images of (a) S1, (b) S4, (c) S5 and (d) S6 nanofibers taken with 25000 magnification after the anisole treatment.

Table 2. Average nanofiber diameters of uniaxial PA6 nanofibers and coaxial nanofibers before and after anisole treatment and reductions (%) in average nanofiber diameter and weight of the nanowebs after anisole treatment.

Samples	Diameter of nanofibers (nm)	Diameter after anisole treatment (core diameter) (nm)	Reduction in diameter by anisole treatment (%)	Reduction in weight by anisole treatment (%)
S1	221.70±21.41	216.84±22.90	2.2	1.5
S4	207.73±18.20	189.41±24.38	8.8	9.3
S5	240.53±31.87	196.42±43.32	18.3	26.4
S6	236.89±35.44	189.12±41.78	20.2	27.1

3. 3 FT-IR Analysis

FTIR analysis was employed to identify the composition of coaxial nanofibers. Pure PA nanofibers and PCL were also characterized for comparison. The spectra of 100% PA 6 and 100% PCL nanofibers were normalized to the largest peaks observed, namely the carbonyl stretchings observed at 1625 cm^{-1} and 1727 cm^{-1} for PA 6 and PCL, respectively. The spectra of multilayered nanofibers were normalized to the absorbance of PA 6 carbonyl peak, which enabled the evaluation of the relative PCL amounts in the coaxial nanofibers. The spectra obtained are presented in Figure 5. For the neat PA 6 nanofibers (Figure 5 (a)), the characteristic bands of secondary amide structure are observed. The absorption bands positioned at 3295 cm^{-1}, 1639 cm^{-1} and 1543 cm^{-1} are due to N-H stretching, C=O stretching, in-plane N-H bending, respectively. The weak band at 3086 cm^{-1} is assigned to the overtone of in-plane N-H bending. Other characteristic bands of secondary amides are C-N stretching which appears from 1310 to 1230 cm^{-1} and out-of-plane N-H stretching which gives rise to a broad, medium-to-weak band from 750 to 680 cm^{-1}. These two peaks were recognized at 1265 and 729 cm^{-1} on PA nanofiber spectrum, respectively [36]. In the spectrum of PCL (Figure 5 (b)), the carbonyl stretching peak at 1723 cm^{-1} is easily identified. The band at 1293 cm^{-1} is assigned to the backbone C–C and C–O stretchings in the crystalline PCL, whereas the band at 1240 cm^{-1} is assigned to asymmetric C–O–C stretching. The sharp band observed at 1169 cm^{-1} represents an overlap of three different bands: namely OC-O stretching (1192 cm^{-1}), symmetric C-O-C stretching (1180 cm^{-1}), amorphous stretching (1162 cm^{-1}) [37-40]. The two peaks observed between 2945 and 2855 cm^{-1} are attributed respectively to the asymmetric and symmetric stretching of CH_2 present in both PA and PCL [41]. On the spectra of PA (core) / PCL (shell) coaxial nanofibers (Figure 5 (c) and (d)), bands associated with both PA and PCL were observed which confirmed the presence of both polymers in the coaxial nanofiber structure. In parallel with literature, it was possible to detect both polymers in the coaxial nanofiber structure [39-45] as the shell thickness of the coaxial nanofibers were less than the penetration depth of the FTIR spectroscope [42] .

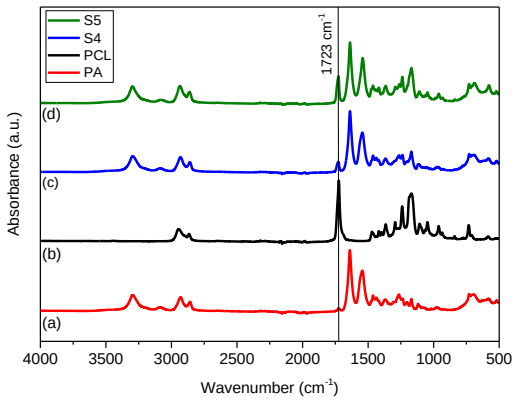

Figure 5. FTIR spectra of (a) S1, (b) PCL (reference), (c) S4 and (d) S5.

The spectra of coaxial nanofibers were normalized to the absorbance intensity of carbonyl band (1637 cm^{-1}) of PA in order to be able to observe the changes in the intensity of the PCL related bands (e.g. carbonyl band at 1723 cm^{-1}). The intensity of the PCL related bands increased as PCL amount increased in the coaxial nanofiber structure (Figure 5 (c) and (d)). A_{1723}/A_{1637} ratio, the absorbance intensity ratios of peaks at 1723 cm^{-1} (carbonyl peak of PA) and 1637 cm^{-1} (carbonyl peak of PCL) were used as an indication of the PA:PCL ratio [15,46]. It increased from 0.167 to 0.444 as the flow rate of the shell solution (PCL) increased from 0.4 to 1.4 ml/min.

Additionally, the nanofiber webs were characterized after PCL extraction by FTIR to confirm the complete removal of PCL. Neat PA nanofibers were also treated with anisole to confirm that PA was not affected by the anisole treatment while the PCL shell was removed. The FTIR spectra of the coaxial nanofiber webs taken before and after anisole treatment are presented in Figure 6. The spectra of PA nanofibers remained unchanged after the anisole treatment (Figure 6(a)). For the PA(core)-PCL(shell) coaxial nanofibers (Figure 6 (b) and (c)), the carbonyl peak (1725 cm^{-1}) (marked with an asterisk on the figures) disappeared after the anisole treatment which confirmed that PCL shell was completely removed and a nanofiber web made of PA 6 was obtained by anisole treatment.

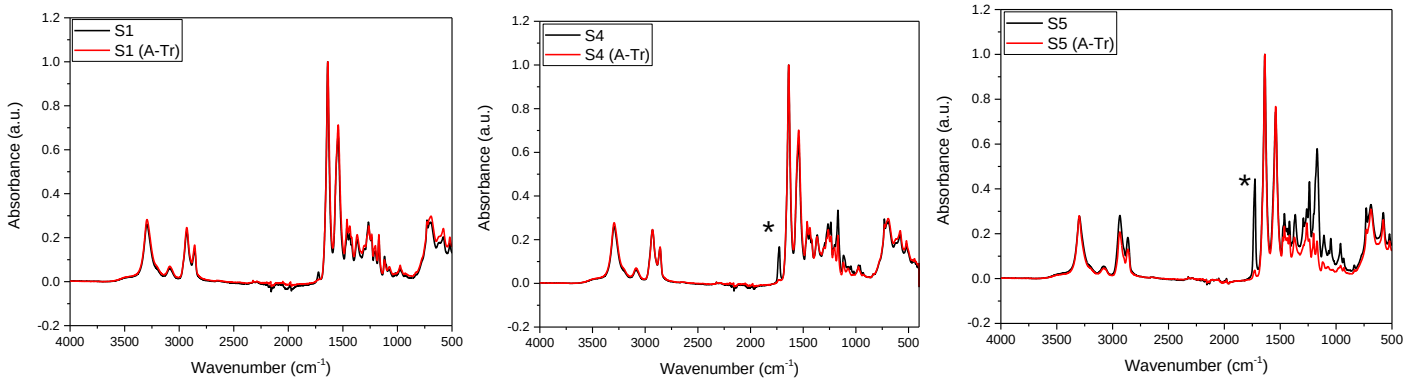

Figure 6. FTIR spectra of (a) S1 (neat PA), (b) S4 and (c) S5 (coaxial) nanofibers before and after anisole treatment. "A-Tr" in the figures shows the anisole treated samples.

3.4 Release profiles

Silver concentration, morphology of the nanofibers, specific surface area of the nanofibers and nanoparticles, and changes in the physical state of a specimen as a result of water diffusion, crosslinking and degree of crystallinity may influence the silver ion release behaviour of materials [25,46-50], which is an important property for silver containing antibacterial materials. It is reported that a steady and prolonged release of silver, with a concentration of above 0.1 ppb, can inhibit the growth of bacteria [23,51].

The silver release profiles of composite uniaxial nanofibers are widely investigated in literature. Shi et al. applied plasma treatment to electrospinning solutions containing $AgNO_3$ for AgNP synthesis and then electrospun PAN/AgNP nanofibers. The cumulative release over 10 days for the $AgNO_3$ concentrations of 0.5% and 1.25% was reported to be approximately 45 and 70 ppm, respectively [22]. Sichani et al. prepared PAN solutions with $AgNO_3$, which were then exposed to light (xenon arc) for 4 h, and electrospun nanofibers after the reduction process. The silver release over 140 hours was reported to be about 0.7 ppm for 0.1 gram PAN nanoweb containing 0.5 wt. % silver nitrate [23].

Silver release profiles of composite PA 6 nanofibers with AgNPs and coaxial nanofibers containing AgNPs in the core have been investigated by atomic absorption spectroscopy over 30 days. The results are shown in Figure 7. The silver ion release started at the first day of immersion and continued during the testing duration of 30 days. The cumulative amounts of released silver were observed to be dependent on the immersion time and the initial $AgNO_3$ concentration. The cumulative release over 30 days for the composite nanofibers electrospun from PA 6 solution containing 1% and 3% $AgNO_3$ was approximately 29 and 79 ppm per gram of nanofibers, respectively. A burst release was observed in the composite nanofibers electrospun from PA 6 solution containing 3 wt. % $AgNO_3$. The burst release was attributed to the tendency of the AgNPs to migrate to the nanofiber surface due to the whipping motion during nanofiber formation [42]. Coaxial nanofibers, in which AgNP containing PA 6 was covered by PCL shell layer, showed much less silver release rates. The increase in the flow rate of the shell solution and concurrent increase in the shell thickness, resulted in further decrease in silver release and also eliminated the burst releases observed for composite nanofibers. The cumulative release for the coaxial nanofibers with PA 6 - 1 wt.% $AgNO_3$ core over 30 days was measured as 19 ppm per 1 g of nanofiber. As far as the burst release and silver release profiles of coaxial nanofibers considered, the results obtained in this study are coherent with literature. Having used $AgNO_3$ as the AgNP precursor and performed nanoparticle synthesis by heating the precursor containing solution for a certain time, Khodkar and Ebrahimi also reported decrease in burst release and silver release rates for coaxial nanofibers of PVA/PCL and PCL/PVA containing AgNPs in the core [42]. The silver release rates, and cumulative release amounts indicated that the multilayered nanofibers were promising for antibacterial applications requiring sustained and controlled release of silver.

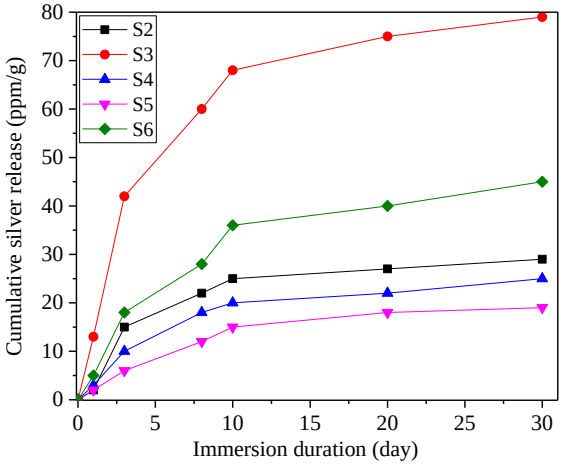

Figure 7. Silver release profiles of AgNP containing uniaxial and coaxial nanofiber samples.

4. CONCLUSIONS

Uniform uniaxial composite PA 6 nanofibers with AgNPs and coaxial PA 6 (core) / PCL (shell) nanofibers containing AgNPs in the core were produced by coaxial electrospinning. UV-Visible spectra showed that the size of nanoparticles were about 10 nm and the content of nanoparticles were observed to be proportional to the precursor content. The multilayered structure of the coaxial nanofibers was confirmed by the selective dissolution and removal of shell layer. The increase in the PCL content with the increase in the flow rate of the shell was confirmed by FTIR. The cumulative silver release of nanofibers decreased when the silver nanoparticles were loaded into the core of the coaxial nanofibers which were covered by the shell PCL layer. Besides, the thickness of the shell layer, which was determined by the flow rate of the shell solution, was also found effective in release properties of the nanofibers. The results obtained showed that the release properties of the nanofibers could be adjusted via changing fiber configuration, precursor content and fiber structural properties such as shell thickness. The multilayered nanofibers providing controlled and sustained release of silver were promising for antibacterial applications.

REFERENCES

1. Fang J, Niu H, Lin T, Wang X (2008) Applications of electrospun nanofibers. Chin Sci Bull 53 (15):2265. doi:10.1007/s11434-008-0319-0

2. Fang J, Wang X, Lin T (2011) Functional Applications of Electrospun Nanofibers. In: T. L (ed) Nanofibers-Production, Properties and Functional Applications. InTechOpen, pp 287-327. doi:10.5772/916

3. Picciani PHS, Medeiros ES, Pan Z, Orts WJ, Mattoso LHC, Soares BG (2009) Development of conducting polyaniline/poly(lactic acid)

nanofibers by electrospinning. J Appl Polym Sci 112 (2):744-753. doi:https://doi.org/10.1002/app.29447

4. Shi X, Zhou W, Ma D, Ma Q, Bridges D, Ma Y, Hu A (2015) Electrospinning of Nanofibers and Their Applications for Energy Devices. Journal of Nanomaterials 2015:140716. doi:10.1155/2015/140716

5. Jiang H, Hu Y, Li Y, Zhao P, Zhu K, Chen W (2005) A facile technique to prepare biodegradable coaxial electrospun nanofibers for controlled release of bioactive agents. J Controlled Release 108 (2):237-243. doi:https://doi.org/10.1016/j.jconrel.2005.08.006

6. Huang ZM, He CL, Yang A, Zhang Y, Han XJ, Yin J, Wu Q (2006) Encapsulating drugs in biodegradable ultrafine fibers through co-axial electrospinning. J Biomed Mater Res A 77 (1):169-179. doi:10.1002/jbm.a.30564

7. Li XY, Li YC, Yu DG, Liao YZ, Wang X (2013) Fast disintegrating quercetin-loaded drug delivery systems fabricated using coaxial electrospinning. Int J Mol Sci 14 (11):21647-21659. doi:10.3390/ijms141121647

8. Mitchell TJ, Keller MW (2013) Coaxial electrospun encapsulation of epoxy for use in self-healing materials. Polym Int 62 (6):860-866. doi:https://doi.org/10.1002/pi.4397

9. Neisiany RE, Khorasani SN, Kong Yoong Lee J, Ramakrishna S (2016) Encapsulation of epoxy and amine curing agent in PAN nanofibers by coaxial electrospinning for self-healing purposes. RSC Advances 6 (74):70056-70063. doi:10.1039/C6RA06434E

10. Hu W, Yu X (2012) Encapsulation of bio-based PCM with coaxial electrospun ultrafine fibers. RSC Advances 2 (13):5580-5584. doi:10.1039/C2RA20532G

11. Ojha SS, Stevens DR, Hoffman TJ, Stano K, Klossner R, Scott MC, Krause W, Clarke LI, Gorga RE (2008) Fabrication and characterization of electrospun chitosan nanofibers formed via templating with polyethylene oxide. Biomacromolecules 9 (9):2523-2529. doi:10.1021/bm800551q

12. Li D, Xia Y (2004) Direct Fabrication of Composite and Ceramic Hollow Nanofibers by Electrospinning. Nano Lett 4:933-938

13. Zussman E, Yarin AL, Bazilevsky AV, Avrahami R, Feldman M (2006) Electrospun Polyaniline/Poly(methyl methacrylate)-Derived Turbostratic Carbon Micro-/Nanotubes. Adv Mater 18 (3):348-353. doi:https://doi.org/10.1002/adma.200501153

14. Merkle VM, Zeng L, Slepian MJ, Wu X (2014) Core-shell nanofibers: Integrating the bioactivity of gelatin and the mechanical property of polyvinyl alcohol. Biopolymers 101 (4):336-346. doi:10.1002/bip.22367

15. Pakravan M, Heuzey M-C, Ajji A (2012) Core–Shell Structured PEO-Chitosan Nanofibers by Coaxial Electrospinning. Biomacromolecules 13 (2):412-421. doi:10.1021/bm201444v

16. Nguyen TTT, Chung OH, Park JS (2011) Coaxial electrospun poly(lactic acid)/chitosan (core/shell) composite nanofibers and their antibacterial activity. Carbohydr Polym 86 (4):1799-1806. doi:https://doi.org/10.1016/j.carbpol.2011.07.014

17. Amiruddin Fadzli Z, Ranganathan B, Sundarrajan S, Ramakrishna S Coaxial electrospun nanofibers as pharmaceutical nanoformulation for controlled drug release. In: 14th IEEE International Conference on Nanotechnology, 18-21 Aug. 2014 2014. pp 531-534. doi:10.1109/NANO.2014.6968190

18. Ibrahim S, Rezk MY, Ismail M, Abdelrahman T, Sharkawy M, Abdellatif A, Allam NK (2020) Coaxial nanofibers outperform uniaxial nanofibers for the loading and release of pyrroloquinoline quinone (PQQ) for biomedical applications. Nanoscale Advances 2 (8):3341-3349. doi:10.1039/D0NA00311E

19. Zupančič Š, Sinha-Ray S, Sinha-Ray S, Kristl J, Yarin AL (2016) Controlled Release of Ciprofloxacin from Core–Shell Nanofibers with Monolithic or Blended Core. Molecular Pharmaceutics 13 (4):1393-1404. doi:10.1021/acs.molpharmaceut.6b00039

20. Kharaghani D, Gitigard P, Ohtani H, Kim KO, Ullah S, Saito Y, Khan MQ, Kim IS (2019) Design and characterization of dual drug delivery based on in-situ assembled PVA/PAN core-shell nanofibers for wound dressing application. Scientific Reports 9 (1):12640. doi:10.1038/s41598-019-49132-x

21. Rai M, Yadav A, Gade A (2009) Silver nanoparticles as a new generation of antimicrobials. Biotechnol Adv 27 (1):76-83. doi:https://doi.org/10.1016/j.biotechadv.2008.09.002

22. Shi Q, Vitchuli N, Nowak J, Caldwell JM, Breidt F, Bourham M, Zhang X, McCord M (2011) Durable antibacterial Ag/polyacrylonitrile (Ag/PAN) hybrid nanofibers prepared by atmospheric plasma treatment and electrospinning. Eur Polym J 47 (7):1402-1409. doi:https://doi.org/10.1016/j.eurpolymj.2011.04.002

23. Sichani GN, Morshed M, Amirnasr M, Abedi D (2010) In situ preparation, electrospinning, and characterization of polyacrylonitrile nanofibers containing silver nanoparticles. J Appl Polym Sci 116 (2):1021-1029. doi:10.1002/app.31436

24. Mahapatra A, Garg N, Nayak BP, Mishra BG, Hota G (2012) Studies on the synthesis of electrospun PAN-Ag composite nanofibers for antibacterial application. J Appl Polym Sci 124 (2):1178-1185. doi:https://doi.org/10.1002/app.35076

25. Kumar R, Münstedt H (2005) Silver ion release from antimicrobial polyamide/silver composites. Biomaterials 26 (14):2081-2088. doi:https://doi.org/10.1016/j.biomaterials.2004.05.030

26. Sheikh FA, Barakat NAM, Kanjwal MA, Chaudhari AA, Jung I-H, Lee JH, Kim HY (2009) Electrospun antimicrobial polyurethane nanofibers containing silver nanoparticles for biotechnological applications. Macromolecular Research 17 (9):688-696. doi:10.1007/BF03218929

27. Wang Y, Li Y, Yang S, Zhang G, An D, Wang C, Yang Q, Chen X, Jing X, Wei Y (2006) A convenient route to polyvinyl pyrrolidone/silver nanocomposite by electrospinning. Nanotechnology 17 (13):3304-3307. doi:10.1088/0957-4484/17/13/037

28. Hong KH (2007) Preparation and properties of electrospun poly(vinyl alcohol)/silver fiber web as wound dressings. Polymer Engineering & Science 47 (1):43-49. doi:https://doi.org/10.1002/ pen.20660

29. Jeong L, Park WH (2014) Preparation and characterization of gelatin nanofibers containing silver nanoparticles. International journal of molecular sciences 15 (4):6857-6879. doi:10.3390/ijms15046857

30. Lee SJ, Heo DN, Moon J-H, Ko W-K, Lee JB, Bae MS, Park SW, Kim JE, Lee DH, Kim E-C, Lee CH, Kwon IK (2014) Electrospun chitosan nanofibers with controlled levels of silver nanoparticles. Preparation, characterization and antibacterial activity. Carbohydr Polym 111:530-537. doi:https://doi.org/10.1016/j.carbpol.2014.04.026

31. Lala NL, Ramaseshan R, Bojun L, Sundarrajan S, Barhate RS, Ying-Jun L, Ramakrishna S (2007) Fabrication of nanofibers with antimicrobial functionality used as filters: protection against bacterial contaminants. Biotechnol Bioeng 97 (6):1357-1365. doi:10.1002/bit.21351

32. Huang L, Zhai ML, Long DW, Peng J, Xu L, Wu GZ, Li JQ, Wei GS (2008) UV-induced synthesis, characterization and formation mechanism of silver nanoparticles in alkalic carboxymethylated chitosan solution. J Nanopart Res 10 (7):1193-1202. doi:10.1007/s11051-007-9353-0

33. Bordes C, Fréville V, Ruffin E, Marote P, Gauvrit JY, Briançon S, Lantéri P (2010) Determination of poly(ε-caprolactone) solubility parameters: Application to solvent substitution in a microencapsulation process. Int J Pharm 383 (1):236-243. doi:https://doi.org/10.1016/j.ijpharm.2009.09.023

34. Zhang W, Qiao X, Chen J (2007) Synthesis of silver nanoparticles—Effects of concerned parameters in water/oil microemulsion. Materials Science and Engineering: B 142 (1):1-15. doi:https://doi.org/10.1016/j.mseb.2007.06.014

35. Wang Y, Yang Q, Shan G, Wang C, Du J, Wang S, Li Y, Chen X, Jing X, Wei Y (2005) Preparation of silver nanoparticles dispersed in polyacrylonitrile nanofiber film spun by electrospinning. Mater Lett 59 (24):3046-3049. doi:https://doi.org/10.1016/j.matlet. 2005.05.016

36. Smith BC (1999) Infrared Spectral Interpretation, A systematic approach. CRC Press, Florid, USA

37. Oliveira JE, Mattoso LHC, Orts WJ, Medeiros ES (2013) Structural and Morphological Characterization of Micro and Nanofibers Produced by Electrospinning and Solution Blow Spinning: A Comparative Study. Advances in Materials Science and Engineering 2013:409572. doi:10.1155/2013/409572

38. Elzein T, Nasser-Eddine M, Delaite C, Bistac S, Dumas P (2004) FTIR study of polycaprolactone chain organization at interfaces. J Colloid Interface Sci 273 (2):381-387. doi:https://doi.org/10.1016/j.jcis.2004.02.001

39. Barati F, Farsani AM, Mahmoudifard M (2020) A promising approach toward efficient isolation of the exosomes by core–shell PCL-gelatin electrospun nanofibers. Bioprocess and Biosystems Engineering 43 (11):1961-1971. doi:10.1007/s00449-020-02385-7

40. Silva JC, Udangawa RN, Chen J, Mancinelli CD, Garrudo FFF, Mikael PE, Cabral JMS, Ferreira FC, Linhardt RJ (2020) Kartogenin-loaded coaxial PGS/PCL aligned nanofibers for cartilage tissue engineering. Materials Science and Engineering: C 107:110291. doi:https://doi.org/10.1016/j.msec.2019.110291

41. Stachewicz U, Hang F, Bailey RJ, Gupta HS, Frogley MD, Cinque G, Barber AH (2012) Recording IR spectra for individual electrospun fibers using an in situ AFM-synchrotron technique. MRS Proceedings 1424:mrsf11-1424-ss1403-1406. doi:10.1557/ opl.2012.151

42. Khodkar F, Golshan Ebrahimi N (2017) Preparation and properties of antibacterial, biocompatible core–shell fibers produced by coaxial electrospinning. J Appl Polym Sci 134 (25). doi:https://doi.org/10.1002/app.44979

43. Xiaoqiang L, Yan S, Rui C, Chuanglong H, Hongsheng W, Xiumei M (2009) Fabrication and properties of core-shell structure P(LLA-CL) nanofibers by coaxial electrospinning. J Appl Polym Sci 111 (3):1564-1570. doi:https://doi.org/10.1002/app.29056

44. Baghali M, Ziyadi H, Faridi-Majidi R (2021) Fabrication and characterization of core–shell TiO2-containing nanofibers of PCL-zein by coaxial electrospinning method as an erythromycin drug carrier. Polym Bull. doi:10.1007/s00289-021-03591-3

45. Movahedi M, Asefnejad A, Rafienia M, Khorasani MT (2020) Potential of novel electrospun core-shell structured polyurethane/starch (hyaluronic acid) nanofibers for skin tissue engineering: In vitro and in vivo evaluation. Int J Biol Macromol 146:627-637. doi:https://doi.org/10.1016/j.ijbiomac.2019.11.233

46. Kumar R, Münstedt H (2005) Polyamide/silver antimicrobials: effect of crystallinity on the silver ion release. Polym Int 54 (8):1180-1186. doi:https://doi.org/10.1002/pi.1828

47. Damm C, Münstedt H (2009) Silver Ion Release from Antimicrobial Acrylate Photopolymer Layers. Polym Polym Compos 17 (9):535-543. doi:10.1177/096739110901700902

48. Radheshkumar C, Münstedt H (2006) Antimicrobial polymers from polypropylene/silver composites—Ag+ release measured by anode stripping voltammetry. React Funct Polym 66 (7):780-788. doi:https://doi.org/10.1016/j.reactfunctpolym.2005.11.005

49. Damm C, Münstedt H, Rösch A (2008) The antimicrobial efficacy of polyamide 6/silver-nano- and microcomposites. Mater Chem Phys 108 (1):61-66. doi:https://doi.org/10.1016/j.matchemphys. 2007.09.002

50. Kumar R, Howdle S, Münstedt H (2005) Polyamide/silver antimicrobials: effect of filler types on the silver ion release. J Biomed Mater Res B Appl Biomater 75 (2):311-319. doi:10.1002/jbm.b.30306

51. Xu X, Yang Q, Wang Y, Yu H, Chen X, Jing X (2006) Biodegradable electrospun poly(l-lactide) fibers containing antibacterial silver nanoparticles. Eur Polym J 42 (9):2081-2087. doi:https://doi.org/10.1016/j.eurpolymj.2006.03.032